Bulletin of the Seismological Society of America, Vol. 98, No. 4, pp. 1737–1749, August 2008, doi: 10.1785/0120070113

Paleoseismology of the Rueisuei Segment of the Longitudinal Valley Fault, Eastern Taiwan

by I-Chin Yen, Wen-Shan Chen, Chih-Cheng Barry Yang, Neng-Wei Huang, and Chii-Wen Lin

Abstract Paleoseismic trench excavations in the Dafu area of eastern Taiwan have provided data on the rupture history of the Rueisuei segment of the Longitudinal Valley fault during the late Holocene. The 1951 Taitung earthquake ruptured the Dafu site, which is characterized by several terrace raises with late Holocene sediments uplifted by the westward thrust fault. Trenches across the northwest-facing fault scarp exposed fluvial and alluvial deposit sediments. Although nearly all of the 23 radiocarbon ages vary somewhat within each layer, the overall age determined for each layer is in good accord with the stratigraphic ordering of these layers. Based on stratigraphic ordering and a statistical comparison of radiocarbon dates using the OxCal program, we estimate that two pre-1951 earthquake surface ruptures at the Dafu site occurred in the periods A.D. 1736–1898 and A.D. 1564–1680. The same OxCal model constrains the past two recurrence intervals to about 165 and 140 yr, although with sizable uncertainties, 55–215 and 90–260 yr, respectively, which are 95% ranges. Through the correlation of three trenches across the Longitudinal Valley fault, we are able to identify evidence for at least three earthquakes with moment magnitudes of about 7.0–7.2 that occurred up to 390 yr prior to and during 1951. Furthermore, based on the radiocarbon dates, the mean recurrence interval is roughly 150 yr (uncertainty is indeterminate), with a minimum vertical uplift rate of 8.5–12.2 mm/yr.

Introduction

The island of Taiwan is the product of the ongoing collision between the Luzon arc and the Chinese continental margin (Chai, 1972; Biq, 1973; Bowin *et al.*, 1978; Teng, 1996; Fig. 1a). The Taiwan orogeny induced by collision started about 4 Ma (Chi *et al.*, 1981; Teng, 1990; Lee and Lawver, 1995). At present, the active collision process is responsible for the highly active seismicity (Wu, 1978; Yu and Tsai, 1982; Tsai, 1986) and rapid crustal movement within and around the area (Chen, 1974; Seno, 1977; Yu *et al.*, 1997). Lying between the two opposing Ryukyu and Luzon arcs, and based on its high level of seismicity, the Longitudinal Valley in eastern Taiwan is considered to be the suture zone of the active collision between the Luzon arc and the Chinese continental margin (Yu and Tsai, 1982; Kao *et al.*, 1998; Rau and Wu, 1998; Chen and Rau, 2002; Kuochen *et al.*, 2005).

The 150-km-long and approximately 4-km-wide Longitudinal Valley of eastern Taiwan lies between the Central Range and the Coastal Range, running from Hualien to Taitung (Fig. 2). The Longitudinal Valley fault is a blind fault under the Longitudinal Valley that dips eastward and separates the Chinese continental margin (the Central Range) to the west and the northernmost segment of the Luzon arc (the Coastal Range) to the east. Based on retriangulation undertaken between A.D. 1909 and 1942 (Chen, 1974) and the retriangulation and collection of leveling data carried out between A.D. 1983 and 1986 (Yu and Liu, 1989), shortening across the Longitudinal Valley fault was estimated to be 2 cm/yr. Several large earthquake ruptures on this fault occurred in 1951 (Hsu, 1962; Bonilla, 1975; York, 1976; Bonilla, 1977; Cheng *et al.*, 1996).

On 24 November 1951, the Taitung earthquake took place, composed of two shocks that occurred at 18:47 and 18:50 UTC. The Yuli and Chihshang faults experienced surface ruptures during these earthquakes. The Yuli fault rupture extended about 43 km, strikes N20°E, and featured oblique left-lateral strike-slip movement. The maximum horizontal displacement was 163 cm, and the eastern block was uplifted 130 cm. The Chihshang fault is also an oblique left-lateral strike-slip fault 5 km away from the Yuli fault, with a rupture length of about 10 km and a strike of N20°E (Hsu, 1962; Bonilla, 1977). Because the surface ruptures were located in remote areas, there was no immediate investigation or detailed mapping of the rupture. The only map of the Taitung earthquake surface ruptures was published more than 10 yr after the earthquake, at a scale of approximately 1:2,000,000

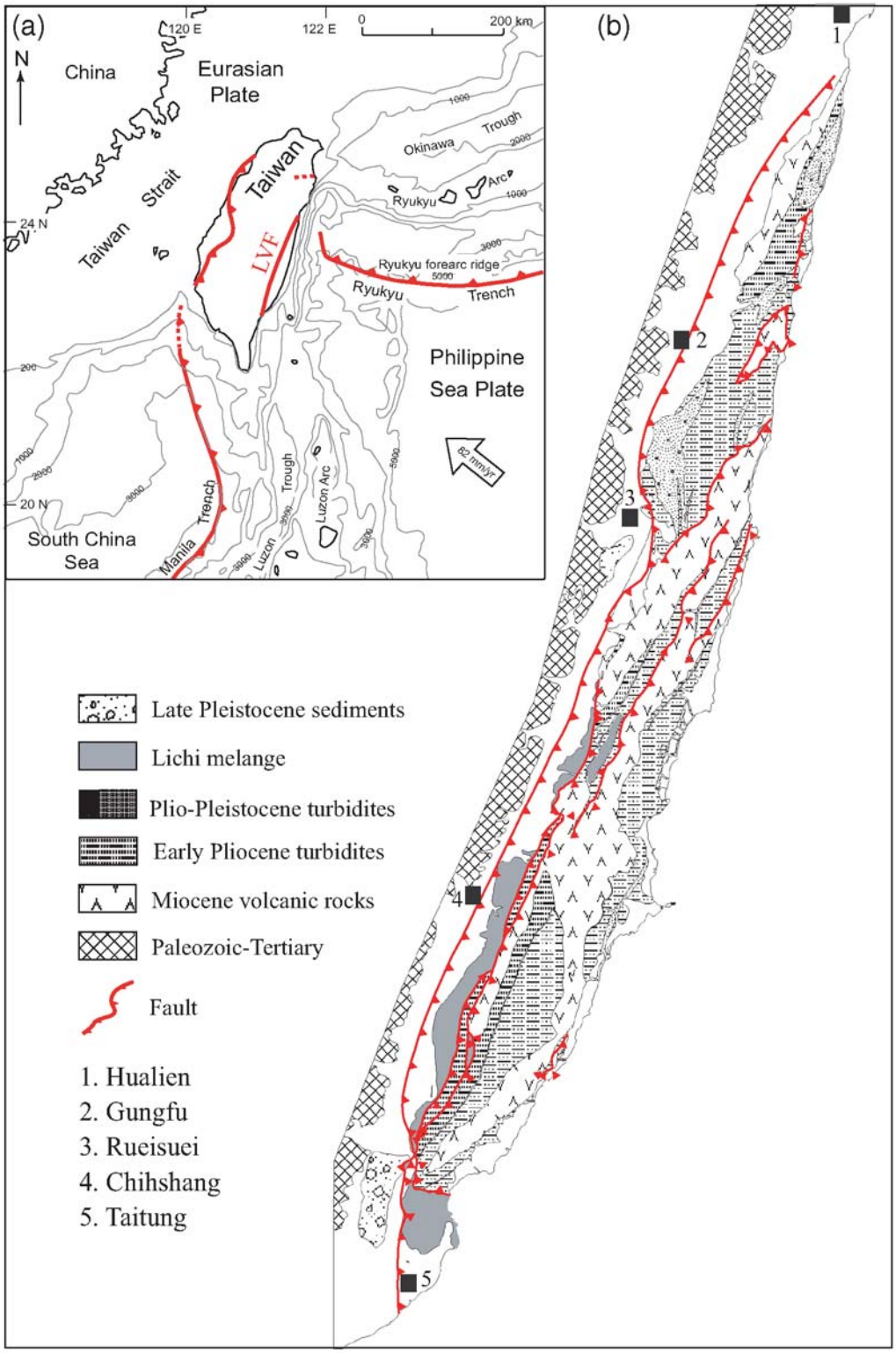

Figure 1. (a) Map showing the tectonic setting surrounding Taiwan. Taiwan orogen is located at the plate boundary between the Philippine Sea plate and the Eurasian plate; LVF: Longitudinal Valley fault. Current velocity vector of the Philippine Sea plate refers to Yu *et al.* (1997). (b) Geological map of the Coastal Range modified from Wang and Chen (1993).

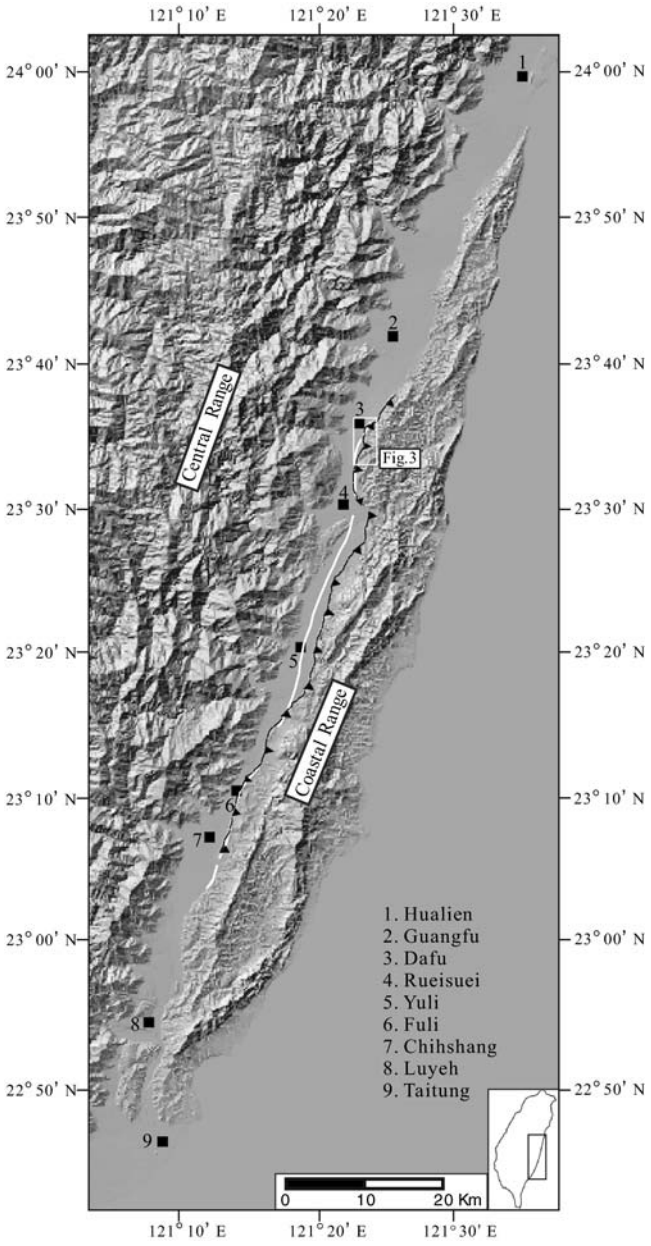

Figure 2. Longitudinal Valley fault map of the study area. The solid black line was the position of the 1951 earthquake ruptures survey undertaken by Hsu (1962), and the white solid lines are the 1951 earthquake ruptures resurvey undertaken by Shyu *et al.* (2007). The location of Figure 3 is also shown.

(Hsu, 1962). More detailed maps of the active structures of the Longitudinal Valley have subsequently been produced (Shyu *et al.*, 2005, 2007).

Taiwan has experienced many destructive earthquakes during the past century (Bonilla, 1975, 1977; Cheng and Yeh, 1989). The 1951 earthquake events occurred within the locality with the highest level of seismicity in Taiwan. These events revealed the fault activity of the suture zone and illustrated the seismic potential of the Longitudinal Valley fault. Before the 1951 Taitung earthquake, there was no direct evidence of surface rupture in the Longitudinal Valley. Our goal is to obtain more information about the behavior of the Longitudinal Valley fault by conducting a paleoseismological study of the rupture zones. In the study reported herein, we excavated four trenches between the towns of Guangfu and Rueisuei, along the central part of the Longitudinal Valley fault, to determine the magnitudes of past earthquakes and the fault's earthquake recurrence time.

Geological Setting of the Longitudinal Valley

The Longitudinal Valley is located between the Coastal Range and the Central Range in eastern Taiwan (Figs. 1 and 2). The Coastal Range is an assemblage of volcanic and siliciclastic rocks accreted within the Luzon arc–trench system (Chen, 1988; Fig. 1b). The Central Range is composed of low-grade metamorphic rock formed in the Mesozoic to Paleogene ages (Ho, 1988). Coarse clastic fluvial sediment (with a thickness of more than 1 km) from the late Quaternary age fills the Longitudinal Valley (e.g., Chen *et al.*, 1974; Chen, 1976).

The east-dipping Longitudinal Valley fault is the dominant neotectonic element in eastern Taiwan. It follows the eastern edge of the valley and accommodates the rapid uplift of the Coastal Range on its hanging-wall block (Hsu, 1954; Hsu *et al.*, 2003). Several large earthquakes occurred in 1951, causing surface ruptures along the fault (Hsu, 1962; Bonilla, 1975; York, 1976; Cheng *et al.*, 1996). According to Angelier *et al.* (1997) and Lee *et al.* (2003), one part of the Longitudinal Valley fault is creeping aseismically at a high rate. Geodetic results indicate that the net horizontal motion across the Longitudinal Valley changes from 34 mm/yr along a section with a trend of 314° at Taitung to 25 mm/yr along the north–south section at Hualien (Yu *et al.*, 1990). Creepmeter measurements reveal that the Longitudinal Valley fault zone is creeping at a rate of about 20 mm/yr near the town of Chihshang (Lee *et al.*, 2001, 2003). Inversion of Global Positioning System (GPS) data across Taiwan also indicates that the Longitudinal Valley fault is a major active structure (Hsu *et al.*, 2003).

In the central Longitudinal Valley, Quaternary alluvial fans and river terraces are well developed and preserved. The principal sources for the Quaternary deposits found within the valley are conglomerates from the Coastal Range and metamorphic rock from the Central Range. Surface ruptures along the Longitudinal Valley fault during the 1951 earthquake series (Hsu, 1962; Shyu *et al.*, 2007) extend approximately 40 km from south of Guangfu to north of Fuli (Fig. 2), with 1.63 m of left-lateral offset and 1.3 m of vertical offset around the Rueisuei area (Hsu, 1955; Shyu *et al.*, 2007). The seismic rupture displaced terraces from Guangfu to Rueisuei. A dense GPS network surveyed from 1996 to 1999 revealed a velocity of 13.3–20.4 mm/yr along a direction varying between 309° and 314° in this area (Yu and Kuo, 2001).

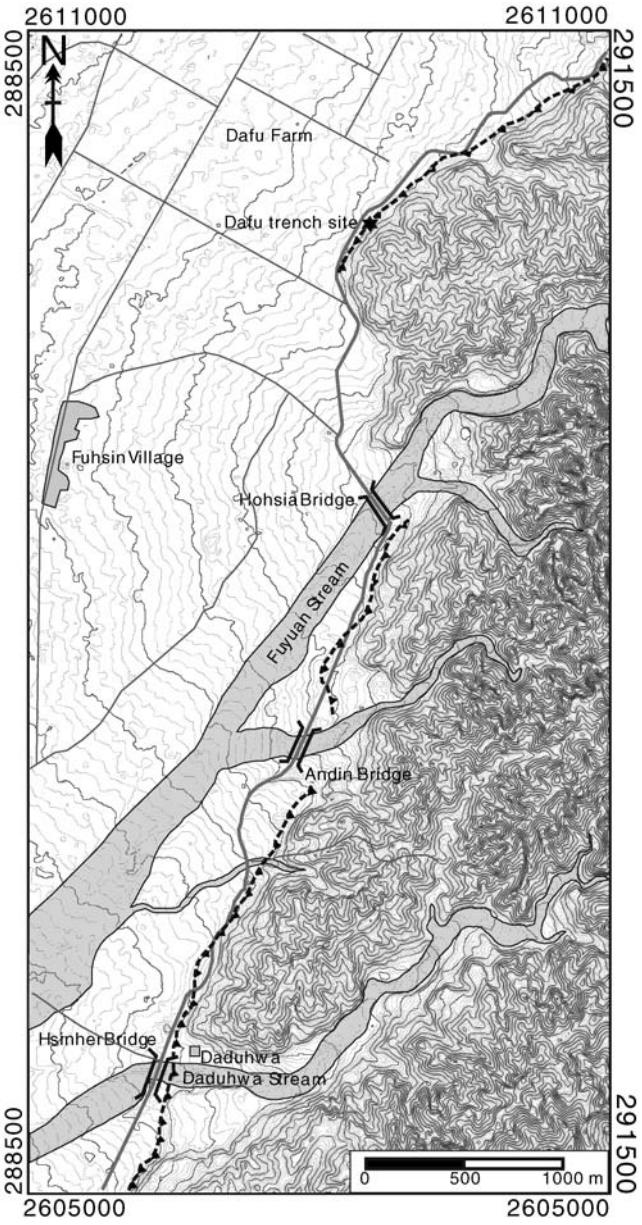

Figure 3. Location map of the Dafu trenches site. The trenches (stars) were excavated across the 1951 earthquake rupture and are located at the northern end of the Fuyuan stream fan. The dotted black line indicates the 1951 earthquake ruptures. The gray line represents Highway 193.

The 1951 Earthquake

Two major shocks occurred at 02:47 and 02:50 (local time) on 25 November 1951 (Taiwan Weather Bureau, 1952) on the Yuli and Chihshang faults, respectively. Cheng *et al.* (1996) used the *S-P* times reported by the Taiwan Weather Bureau to relocate the epicenter using a Monte Carlo algorithm. The length of the surface fault rupture and the maximum ground-motion amplitudes were applied to reevaluate the magnitude of these two events. They placed the hypocenter of the first shock at 23.100°N and 121.225°E, with a depth of 16 km and a magnitude of M_w 6.2. The hypocenter of the second shock was located at 23.175°N and 121.350°E at a depth of 36 km, with a magnitude of M_w 7.0. They also derived focal mechanisms by combining the first *P* motion reported by the Taiwan Weather Bureau (1952) with geological data recorded in Hsu's (1962) map. They conclude that the first shock was a thrust fault with a left-lateral strike-slip component (strike, N32°E; dip, 70° SE; and rake, 70°) and that the second shock was a left-lateral strike slip with a thrust fault component (strike, N25°E; dip, 70° SE; and rake, 40°). These two shocks caused 17 fatalities and seriously injured 326, while destroying 1016 houses and partly damaging 582 others from the village of Wulou (3.8 km north of Rueisuei) to Chihshang.

Shyu *et al.* (2007) reevaluated the 1951 earthquake ruptures by analyzing published documents, relevant reports, and photographs and by interviewing more than 40 elderly local residents who experienced the earthquakes. Based on this reevaluation, they divided the surface ruptures into three sections from south to north—the Chihshang, Yuli, and

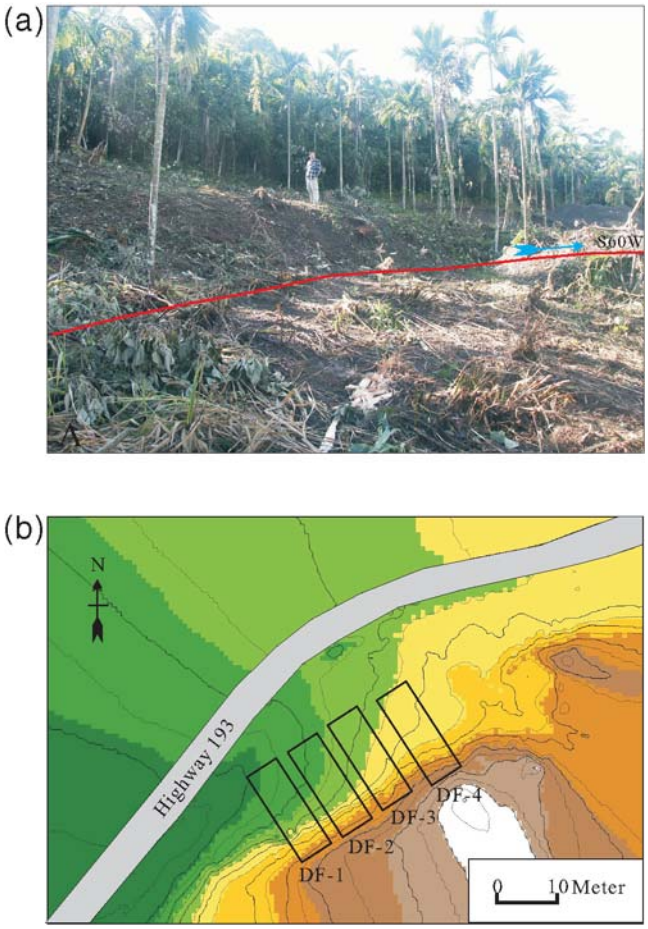

Figure 4. (a) Photo of the Dafu site fault scarp before excavation looking in a southeasterly direction. The height of the man on the hanging wall is 180 cm. The red line indicates the 1951 earthquake surface rupture trending S60°W. (b) Topography around the trench sites. Contour interval of 1 m.

Table 1
Summary of Radiocarbon Analyses, Dafu Site, Eastern Taiwan

Sample Number	Laboratory Number	Stratigraphic Unit	Description	Radiocarbon Age* (yr B.P.)	Calendar Date† (yr A.D. 2σ)	Calibrated Age‡ (yr A.D. 2σ)
DAF-36	Beta-202143	T	Charcoal	176.0 ± 0.5 pMC	later 1950	1954–1978
DAF-74	Beta-202145	T	Charcoal	113.3 ± 0.5 pMC	later 1950	1951–1981
Event El						1951
CLK-066	Beta-190954	S2	Charcoal	270 ± 40	1523–1795	1785–1950
CLK-037	Beta-190952	S2	Charcoal	140 ± 40	1676–1941	1806–1945
CLK-011	Beta-190950	S2	Charcoal	260 ± 40	1524–1798	1785–1950
CLK-035	Beta-190951	S2	Charcoal	230 ± 40	1641–1950	1782–1950
CLK-089	Beta-190955	S2	Charcoal	200 ± 50	1650–1950	1778–1950
CLK-056	Beta-190953	S2	Charcoal	130 ± 30	1683–1936	1836–1938
CLKN-017	Beta-207690	S2	Charcoal	130 ± 40	1682–1937	1836–1941
Event E2						1748–1849
DAF-45	Beta-202144	O1	Charcoal	250 ± 40	1527–1950	1640–1796
DF-05	Beta-190961	O1	Charcoal	270 ± 40	1523–1795	1638-1791
DF-04	Beta-190960	O1	Charcoal	200 ± 40	1655–1950	1654–1775
DF-03	Beta-190959	O1	Charcoal	230 ± 40	1641–1950	1644–1794
DAF-13	Beta-202140	O1	Charcoal	150 ± 40	1669–1945	1669–1771
DAF-30	Beta-202142	O1	Charcoal	140 ± 40	1676–1941	1674–1764
DAF-20	Beta-202141	O1	Charcoal	160 ± 40	1668–1950	1667–1775
DAF-05	Beta-202139	O1	Charcoal	120 ± 40	1684–1929	1680–1761
DAF048	Beta-207694	O1	Charcoal	170 ± 40	1665–1950	1666–1776
DAF051	Beta-207695	O1	Charcoal	60 ± 40	1697–1917	1692–1729
DAF053	Beta-207696	O1	Charcoal	220 ± 40	1645–1950	1647–1788
Event E3						1622–1664
CLKN-18	Beta-190957	O2	Charcoal	270 ± 40	1523–1795	1545–1655
CLKN-101	Beta-190958	O2	Charcoal	280 ± 40	1521–1662	1548–1654
CLKN-07	Beta-190956	O2	Charcoal	310 ± 40	1516–1645	1569–1649

*Radiocarbon ages were measured using accelerator mass spectrometry by Beta Analytic, Inc.
†Calendar age dendrochronologically calibrated by method A from the program of Reimer *et al.* (2004), with 2 standard deviation uncertainty.
‡Calibrated using OxCal Program 4.0.5 (Ramsey, 2007).

Rueisuei sections. The Chihshang section is approximately 30 km long and probably ruptured during the first shock of the 1951 earthquake series. The length of the Yuli rupture is about 20 km, and the Rueisuei rupture is about 15 km long; both ruptures were probably produced by the second shock of the 1951 series. They concluded that the Chihshang rupture, which produced the first shock, probably triggered the subsequent failure of the Yuli and Rueisuei ruptures. They also consider that the northern end of the Rueisuei rupture is near the Tzu-Chiang Prison (about 10 km south of the town of Kuangfu) and that the southern end is near the village of Hekang (about 2 km east of the town of Rueisuei), extending about 15 km along the western foothills of the Coastal Range. Along the rupture, most of the rupture scarps are still visible, allowing us to select places to trench.

Geomorphic Framework of the Trench Area

Fuyuan stream is the largest stream in the study area that flows from the Coastal Range (Fig. 3). From Dafu Farm to Daduhwa village, the stream formed Holocene alluvial fans 5 km in length and 1 km in width in the central area of the Longitudinal Valley. Daduhwa stream flows from the Coastal Range and merges with the Fuyuan stream southwest of Daduhwa village. Aside from these two streams, a few intermittent streams also supply sediments to the alluvial fan. Several uplifted stream terraces, which are about 2–3 m higher that the alluvial fan, run along the mountain streams and cross the fans with a distinct fault scarp running in a north-northeast–south-southwest direction.

We reinvestigated the reported 1951 rupture and mapped the surface rupture in greater detail. We found that the 1951 earthquake rupture was along the reported north-northeast–south-southwest trending fault scarp and recorded about 1.2 m of height in this area. However, we also found a surface rupture that had not previously been mapped. This newly discovered surface rupture displaces the eastern terrace rise by about 2 m (Fig. 4). At this location, we excavated four trenches across and perpendicular to the surface rupture trace.

Radiocarbon Dating

We collected detrital charcoal in the trenches. Samples for radiocarbon dating were analyzed by Beta Analytic, Inc. (Miami, Florida). A total of 23 charcoal fragment samples were dated by accelerator mass spectrometry (Table 1). All samples are detrital, so they represent the maximum ages for the sedimentary layers from which they were collected, because the samples may have already had a significant radiocarbon age at the time they were deposited. These analyses suggest that the composite stratigraphic record at the Dafu site extended from at least A.D. 1500 to the present.

We assume that the charcoal incorporated into each deposit was derived from the ground surface or near-surface soil directly uphill from the depositional site and that the 2σ range in calibrated age adequately reflects the maximum deposit age. Therefore, the youngest radiocarbon date from each unit should best represent the maximum deposit age.

Based on this approach, a total of 23 samples yielded representative ages (Fig. 5), and these dates were used in the OxCal calibration and analysis program (Ramsey, 1995, 2001, 2007) to help interpret the ages of the deposits and timing of earthquake events at the Dafu site. This program uses stratigraphic relations among deposits and Bayesian statistics applied to deposit ages to develop probability density functions for the ages of interdeposit events. The laboratory ages of these deposits were calibrated to the tree-ring record using the OxCal program (version 4.0.5; Ramsey, 2007) and were then used to construct an analytical model that consists of four separate depositional phases encompassing the three earthquake events.

Paleoseismology Analysis

Sequence of Events and Rupture Displacement

We excavated four trenches, each about 20 m long, 6 m deep, and 8 m wide (DF-1, DF-2, DF-3, and DF-4) across the fault scarp at the Dafu site (Fig. 4b). The Longitudinal Valley fault at the margin of the Coastal Range displaces the Pleistocene conglomerate and Holocene alluvial deposits. The trench walls showed intense folding in the hanging wall, related to four reverse fault strands (Fc1, Fc2, Fc3, and Fc4). The exposed sediment is predominately composed of alluvial and colluvial deposits and two organic-rich silty layers (units O2 and O1; Fig. 6). The lower units G1 and G2 are stratified gravels with lenticular sand layers of alluvial deposits. The matrix of unit G1 is muddier than unit G2, and the gravel deposits of unit G1 are larger than those of unit G2. Unit S2 consists of matrix-supported gravels deposited as colluvium on the fault scarp. Unit S1 consists of planar laminated fine sand, interpreted to be a fluvial deposit, forming a flood plain on the fault scarp.

On the basis of cross-cutting relations, event E1 along faults Fc1 and Fc4 occurred after deposition of unit S2 but before unit T. The displacement of fault Fc1 is thus interpreted to have been caused by the 1951 earthquake (Fig. 6). The vertical displacement of Fc1 in trench DF-4 is about 1.5 m (Fig. 6h). The vertical displacement of fault Fc1 in the northern wall of trench DF-2 is 1.7 m as defined by the offset of unit S2 (Fig. 6d, A to A′), whereas the bottom of unit O1 displays a vertical displacement of at least 3 m across the same fault (Fig. 6c, B to B′). These observations indicate that fault Fc1 has been subject to at least two events, which we refer to as the E1 event (the 1951 earthquake) and the Ena event (older). The restoration of the offset of the 1951 earthquake still gives a vertical displacement for fault Fc1 of 1.3 m, and unit G2 retains warping and overlapping

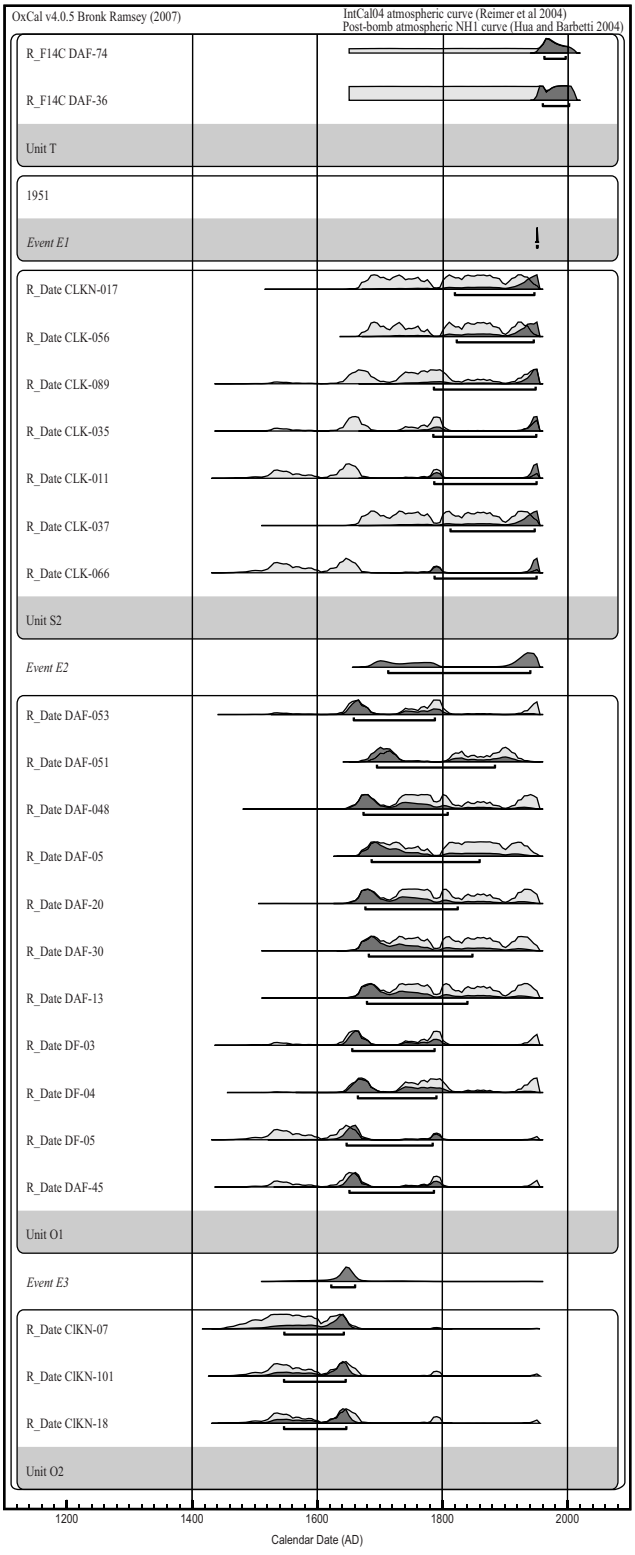

Figure 5. Results of the OxCal analysis of radiocarbon dates. Open curves represent the prior probability distribution. Filled curves represent the posterior distributions. The boundaries mark contacts between channels and earthquake horizons. The number after each radiocarbon date is the agreement index, indicating the extent of overlap between the prior and posterior distributions.

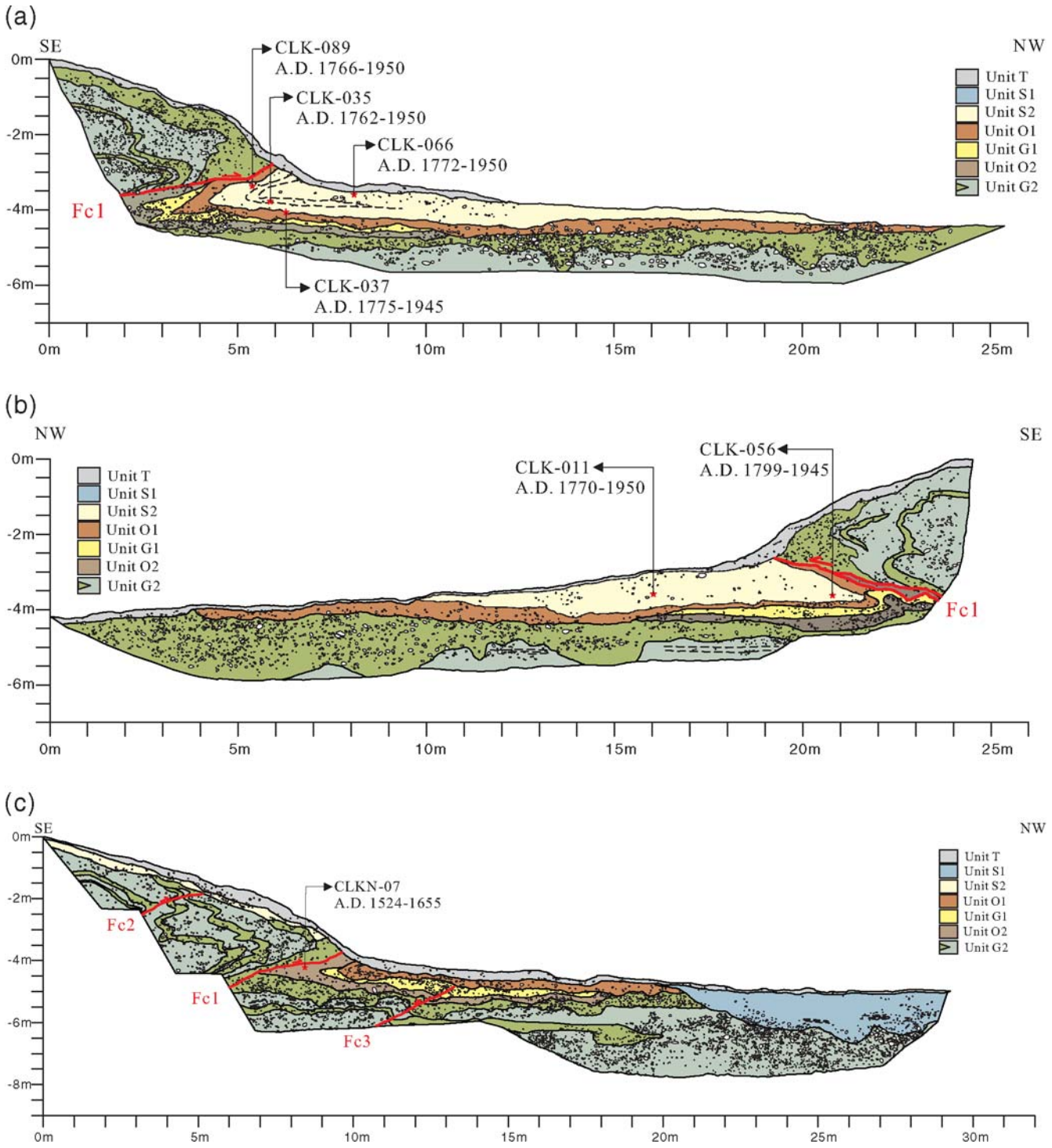

Figure 6. (a) Map of the southern wall of trench 1. (b) Map of the northern wall of trench 1. (c) Map of the southern wall of trench 2. (d) Map of the northern wall of trench 2. The inset, d′, is a detailed map of event E2 of the northern wall of trench 2. (e) Map of the southern wall of trench 3. (f) Map of the northern wall of trench 3. (g) Map of the southern wall of trench 4. (h) Map of the northern wall of trench 4. The dates indicate the 2σ calendrical age range for each sample, based upon accelerator mass spectrometry radiocarbon analyses (Table 1). (*Continued*)

on unit O2, which indicates that the Ena event occurred after the deposition of unit O2. We propose that fault Fc1 represents slippage from two events: 1.7 m in 1951 and 1.3 m from an older event (Ena).

The E2 event was preserved by a deformation event. Unit O1 between Fc3 and Fc1 in the north wall of DF-2 was deformed and covered by the undeformed unit S2, the deformation causing a 0.3-m vertical displacement of unit

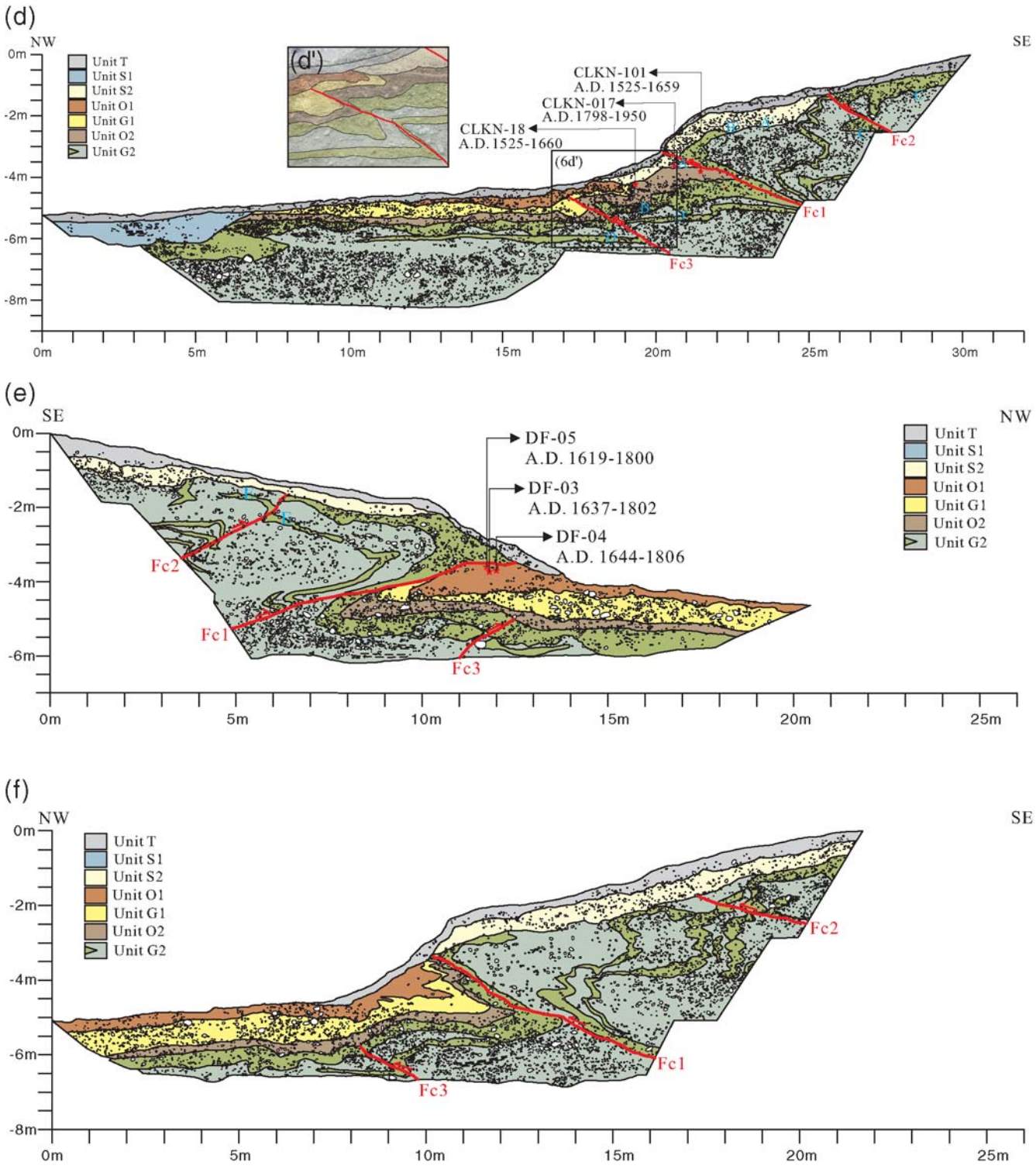

Figure 6. Continued.

O2 (Fig. 6d and the inset d′). Thus, the E2 event must have occurred after the deposition of unit O2 and before the deposition of unit S2.

The E3 event was responsible for the displacement of unit G1 along fault Fc3 and is also covered by the undeformed unit O1 (Fig. 6c–6f). The average vertical displacement of unit O2 across fault Fc3 is 0.6 m (Fig. 6d, D to D′).

Unit G2 in the trenches DF-2 and DF-3 appears to have been displaced by fault Fc2 in the hanging wall (Fig. 6g), and the fault tip is covered by the undeformed unit S2 (Fig. 6c,

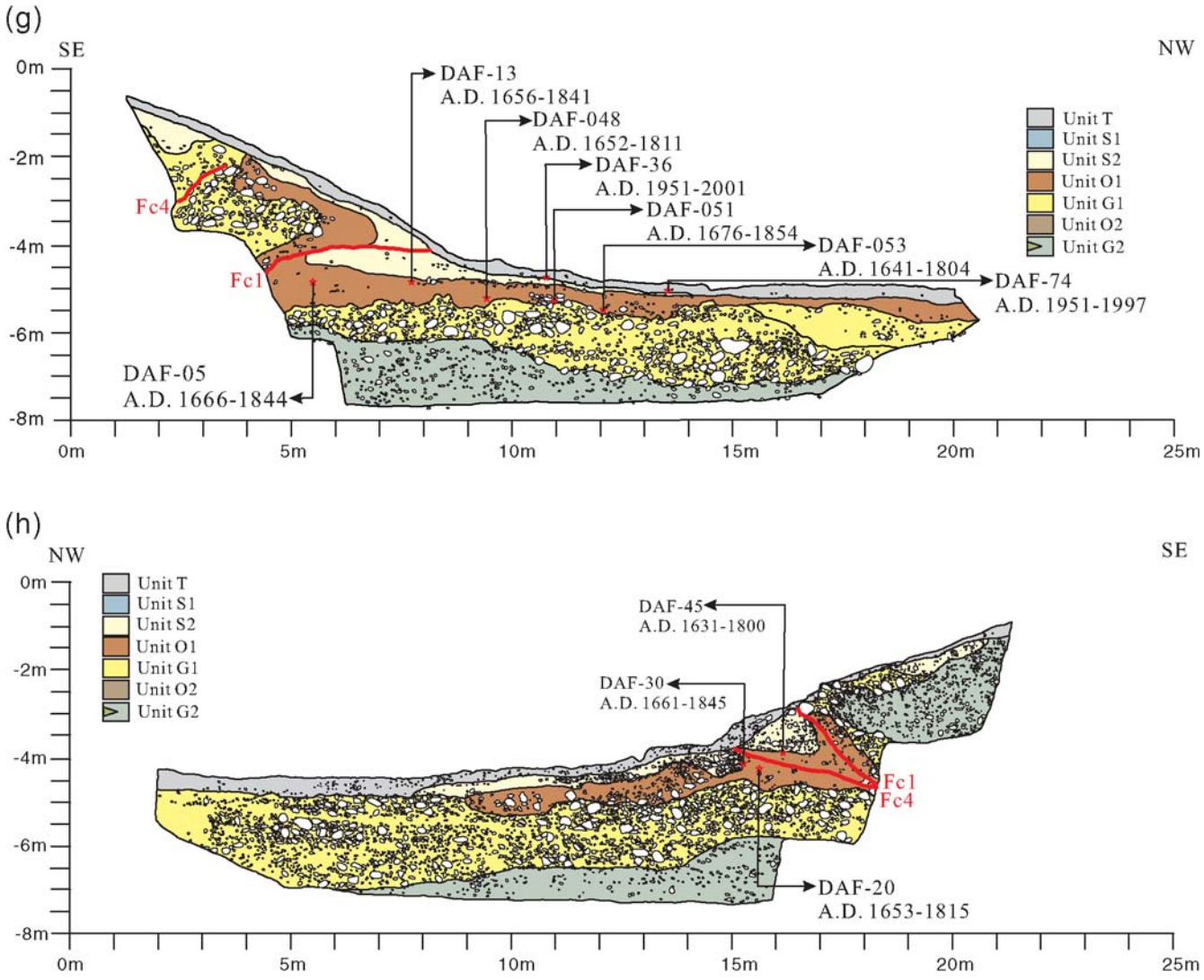

Figure 6. Continued.

6e, and 6f). Thus, the Enb event must have occurred after the deposition of unit G2 and before the deposition of unit S2 by fault Fc2. The average vertical displacement of unit G2 across the fault Fc2 is 1 m (Fig. 6d, C to C′).

The stratigraphic relationships show the E2 and Ena displacements to have occurred after the deposition of unit O2, but there is no way to distinguish between the two events. On the assumption that each event was similar in terms of vertical displacement, we believe the two deformations probably occurred during the same episode of faulting and can determine that the extent of vertical displacement that occurred as a result of the E2 event was 1.6 m. Here, we also believe that the E3 event and the Enb event occurred at the same time. Hence, the E3 event caused a vertical displacement of 1.6 m.

Consequently, the evolution model of the fault active in the Dafu trench site is as shown in Figure 7. First, unit G1 was deposited after unit O2 and unit G2. The E3 event occurred after unit G1 was deposited with fault strands Fc2 and Fc3 and caused a vertical displacement of 1.6 m. After the E3 event, unit O1 was deposited following an erosion process. Immediately thereafter, the fault strand Fc1 was cut through O1 and caused the deformation in front of fault strand Fc1 during the E2 event, resulting in a total vertical displacement of 1.6 m. Finally, the 1951 event (E1) occurred after the unit S2 deposit on the erosion surface and was covered by unit T.

Paleoearthquake Timing

Based on radiocarbon dates estimated using the Bayesian approach and the paleoseismological event sequence, we propose the paleoearthquake timing for this fault segment. Assuming that the three stratigraphically consistent radiocarbon ages of the detrital charcoal samples (CLKN07, CLKN18, and CLKN101) represent the depositional ages of unit O2, we interpret the depositional age of unit O2 to be A.D. 1524–1660. Based on the 11 detrital charcoal sam-

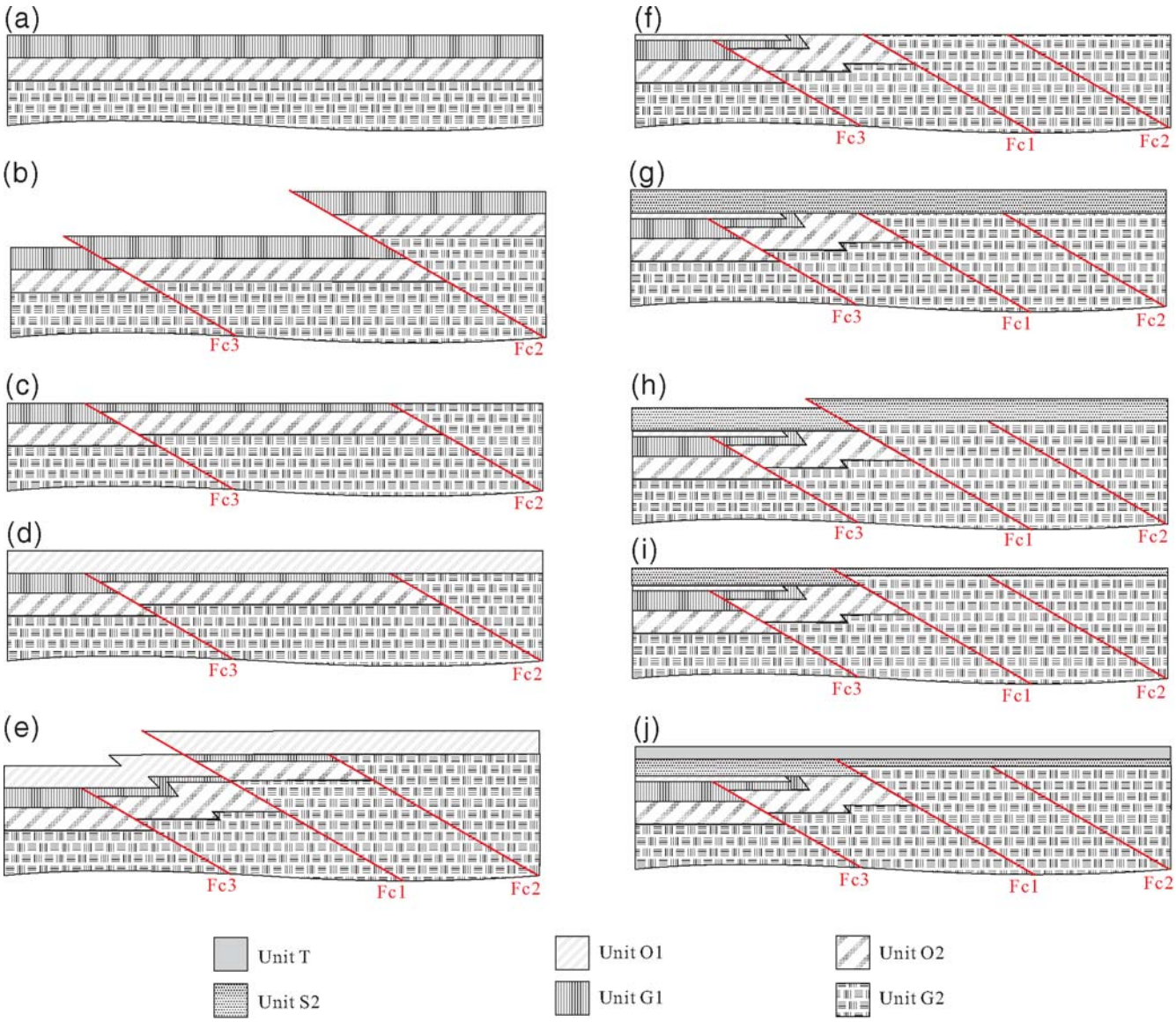

Figure 7. Active fault history of the central part of the Longitudinal Valley fault at the Dafu paleoseismic site over the past 330 yr. (a) Unit G2, unit O2, and unit G1 were deposited in sequence. (b) Fault Fc2 and fault Fc3 cut through unit G1 during event E3 and caused a vertical displacement of 1.6 m. (c) Erosion after event E3. (d) Unit O1 was deposited on the surface after erosion. (e) Fault Fc1 cut through unit O1 and caused deformation at the footwall during event E2, which caused a vertical displacement of 1.6 m. (f) Erosion after event E2. (g) Unit S2 was deposited on the surface after erosion. (h) Fault Fc1 became active again and cut through unit S2 during event E1 in A.D. 1951, causing a vertical displacement of 1.7 m. (i) Erosion after event E1. (j) Unit T was deposited on the surface after erosion.

ples (DAF05, DAF013, DAF020, DAF030, DAF045, DAF048, DAF051, DAF053, DF03, DF04, and DF05), we calculate the depositional age for unit O1 to be A.D. 1619–1854. Based on the seven detrital charcoal samples (CLK011, CLK035, CLK037, CLK056, CLK066, CLKN017, and CLKN089), the depositional age of unit S1 is A.D. 1762–1950. Finally, based on two detrital charcoal samples (DAF36 and DAF74), the depositional age of unit T, the youngest unit, is later than A.D. 1951.

The E1 event is the 1951 earthquake. The E2 event must have occurred after the deposition of unit O1 and before the deposition of unit S2, that is, between A.D. 1736 and 1898, based on the Bayesian approach. The E3 event was responsible for the displacement of unit G1, yet is covered by undeformed unit O1, which indicates the E3 event occurred between the deposition of unit G1 and unit O1. The lack of dates for unit G2 prevents us from defining the upper chronological limit, but using the dates calculated under the Bayesian approach, we estimate that the E3 event occurred between A.D. 1564 and 1680.

Recurrence Time

Based on the chronological constraints in each trench for the paleoearthquakes, we attempted to correlate events between these four trenches (Fig. 7). At least three earthquake

Table 2
Ages of Earthquakes, Dafli Site, Eastern Taiwan

Event	Age Ranges (yr A.D.) 68%	95%	Mean Age* (yr A.D.)	Mean Interval† (yr)	Interval Range (95%)
E1	1951	1951	1951		
				167	56–216
E2	1748–1894	1736–1898	1784		
				141	91–258
E3	1622–1664	1564–1680	1643		

*Derived from the probability density function output from OxCal for each event, as the sum of all products of each date bin and its associated probability. Calibration curve used: IntCal04, Northern Hemisphere (Reimer, *et al.*, 2004).

†Calculated as the difference in mean ages of the events.

events have occurred in the past 390 yr. The most recent event is the 1951 earthquake observed in all four trenches. The earliest event is E3, which probably occurred between A.D. 1564 and 1680 (95% confidence range). E2 probably occurred between A.D. 1736 and 1898 (95% confidence range). Using OxCal, we calculate the earlier recurrence interval to be 91–158 yr (95% confidence range) and the later interval to be 56–216 yr. The mean recurrence interval for the past 390 yr is about 150 yr (Table 2), but error statistics for the mean were not resolvable in OxCal, probably because there are only two intervals and the errors of each are relatively large.

Vertical Uplift Rate

In Figure 8, the solid line shows the vertical offset of each event in the vertical dimension and represents the age constraints of the events with 2σ uncertainties in the horizontal dimension. According to the estimated displacement and the calculated occurrence interval, we can delineate the average yearly vertical uplift rate as the slope of dashed lines, which is between 8.5 and 12.2 mm/yr during the past 390 yr.

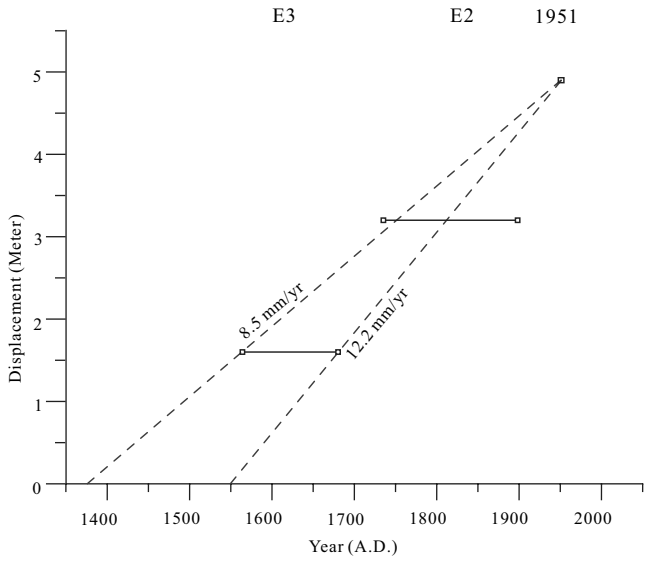

Figure 8. Tentative vertical offset history of the Dafu paleoseismic site over the past 390 yr. The vertical dimension indicates the vertical offset. The horizontal dimension represents the age constraints of the events with 2σ uncertainties. The average uplift rate of 8.5–12.2 mm/yr is shown as the slope of the dashed lines for reference.

Discussion

Slip Rate Estimation

We were unable to determine the fault slip direction from the trenches. However, through a combination of the fault dipping angle and the vertical uplift rate, we can calculate a more accurate fault slip rate using trigonometry. Based on the 30° dipping angle of the fault and a vertical uplift rate of between 8.5 and 12.2 mm/yr, we obtain a slip rate of 17.0–24.4 mm/yr. This slip rate is very similar to the longer term slip rate of the Longitudinal Valley fault (22.7 mm/yr) obtained from the Holocene uplift rate of terraces along the Hsiukuluan River (Shyu *et al.*, 2006). Therefore, we propose that the interseismic stress accumulation is totally released by a coseismic rupture. The Longitudinal Valley fault at this segment seems to be locked during interseismic periods.

Magnitude of the Paleoearthquakes

The magnitude of a paleoearthquake can be estimated from fault displacement. Wells and Coppersmith (1994) obtained relationships of average displacement to moment magnitude from published reports of documented historical surface ruptures. Using data from all types of faults, they found that moment magnitude (M) and average displacement (AD) are related as follows:

$$M = (6.93 \pm 0.05) + (0.82 \pm 0.10) \times \log(\mathrm{AD}).$$

The average displacement of the 1951 earthquake (E1) was 1.7 m, which corresponds to a moment magnitude, M, of 7.1 ± 0.1. The average displacements of the E2 and E3 events were both 1.6 m, which corresponds to a moment magnitude (M) of 7.1 ± 0.1. Thus, the moment magnitudes of the paleoearthquakes at the Dafu site were about 7.0–7.2.

Conclusions

From the paleoseismological record of the Longitudinal Valley fault at the Dafu site, four reverse fault strands with three paleoearthquake ruptures occurred in A.D. 1951 and in the periods A.D. 1736–1898 and A.D. 1564–1680. The mean occurrence interval for the past 390 yr at the Dafu site is approximately 150 yr, and the slip rate is 17.0–24.4 mm/yr. Based on the empirical relationships of magnitude and surface displacement, the moment magnitudes of the paleoearthquakes were about 7.0–7.2.

Acknowledgments

We thank L. H. Liu, Y. C. Chen, K. J. Tsai, and Y. K. Chu for their help with the fieldwork. We are also grateful for valuable discussions with J. B. H. Shyu and K. H. Kang. The comments and suggestions of reviewers J. J. Lienkaemper and R. van Arsdale helped us to greatly improve this manuscript. We would like to thank Christopher Ramsey for providing the OxCal program and code. This work was supported by the Central Geological Survey (MOEA) with Grant Number CGS-5226902000-94-01 and by the Taiwan Earthquake Research Center (TEC) funded through the National Science Council (NSC) with Grant Number NSC-94-2119-M-002-023. The TEC contribution number for this article is 00030.

References

Angelier, J., H. T. Chu, and J. C. Lee (1997). Shear concentration in a collision zone: kinematics of the active Chihshang fault, Longitudinal Valley, eastern Taiwan, *Tectonophysics* **247,** 117–144.

Biq, C. (1973). Kinematic pattern of Taiwan as an example of actual continental-arc collision, *Rep. Seminar on Seismology, US-ROC Cooperative Science Program*, 21–26.

Bonilla, M. G. (1975). A review of recently active faults in Taiwan, *U.S. Geol. Surv. Open-File Rept. 75-41*, 58 pp.

Bonilla, M. G. (1977). Summary of Quaternary faulting and elevation changes in Taiwan, *Mem. Geol. Soc. China* **2,** 43–56.

Bowin, C., R. S. Lu, C. S. Lee, and H. Schouten (1978). Plate convergence and accretion in Taiwan-Luzon region, *Am. Assoc. Petrol. Geol. Bull.* **62,** 1645–1672.

Chai, B. H. T. (1972). Structure and tectonic evolution of Taiwan, *Am. J. Sci.* **272,** 389–422.

Chen, C. Y. (1974). Verification of the north-northeastward movement of the Coastal Range, eastern Taiwan, by re-triangulation, *Bull. Geol. Surv. Taiwan* **24,** 119–123 (in Chinese with English abstract).

Chen, J. S. (1976). The analysis and design of refraction and reflection seismic survey of the Taitung area, *Petrol. Geol. Taiwan* **13,** 225–246.

Chen, W. S. (1988). Tectonic evolution of sedimentary basins in Coastal Range, Taiwan *Ph.D. Thesis*, National Taiwan University, Taipei, 304 pp. (in Chinese).

Chen, H., and R. Rau (2002). Earthquake locations and style of faulting in an active arc-continent plate boundary: the Chihshang fault of eastern Taiwan (Abstract T61B-1277), *EOS Trans. AGU* **83,** no. 47 (Fall Meet. Suppl.), T61B-1277.

Chen, J. S., J. N. Chou, Y. C. Lee, and Y. S. Chou (1974). Seismic survey conducted in eastern Taiwan, *Petrol. Geol. Taiwan* **11,** 147–163.

Cheng, S. N., and Y. T. Yeh (1989). Catalog of the earthquakes in Taiwan from 1604 to 1988, Institute of Earth Sciences, Academia Sinica, Taipei, 255 pp. (in Chinese).

Cheng, S. N., Y. T. Yeh, and M. S. Yü (1996). Determination of earthquake source parameters using a Monte Carlo algorithm, *J. Geol. Soc. China* **39,** 267–285.

Chi, W. R., J. Namson, and J. Suppe (1981). Stratigraphic record of plate interactions in the Coastal Range of eastern Taiwan, *Mem. Geol. Soc. China* **4,** 155–194.

Ho, C. S. (1988). An Introduction to the Geology of Taiwan, Explanatory Text of the Geologic Map of Taiwan, Second ed., Cent. Geol. Surv., Ministry Econ. Affairs, Taipei, 192 pp.

Hsu, T. L. (1954). On the geomorphic features and the recent uplifting movement of the Coastal Range, eastern Taiwan, *Bull. Geol. Surv. Taiwan* **7,** 9–18.

Hsu, T. L. (1955). Earthquakes in Taiwan, *Quart. J. Bank Taiwan* **7,** no. 2, 148–164 (in Chinese).

Hsu, T. L. (1962). Recent faulting in the Longitudinal Valley of eastern Taiwan, *Mem. Geol. Soc. China* **1,** 95–102.

Hsu, Y. J., M. Simons, S. B. Yu, L. C. Kuo, and H. Y. Chen (2003). A two-dimensional dislocation model for interseismic deformation of the Taiwan mountain belt, *Earth Planet. Sci. Lett.* **211,** 287–294.

Kao, H., S. J. Shen, and K. F. Ma (1998). Transition from oblique subduction to collision: Earthquakes in the southernmost Ryukyu arc-Taiwan region, *J. Geophys. Res.* **103,** 7211–7229.

Kuochen, H., Y. M. Wu, C. H. Chang, J. C. Hu, and W. S. Chen (2005). Relocation of the Eastern Taiwan earthquakes and its tectonic implications, *Terr. Atmos. Ocean. Sci.* **15,** 647–666.

Lee, T. Y., and L. A. Lawver (1995). Cenozonic plate reconstruction of Southeast Asia, *Tectonophysics* **251,** 85–138.

Lee, J.-C., J. Angelier, H.-T. Chu, J.-C. Hu, and F.-S. Jeng (2001). Continuous monitoring of an active fault in a plate suture zone: a creepmeter study of the Chihshang fault, eastern Taiwan, *Tectonophysics* **333,** 219–240.

Lee, J. C., J. Angelier, H. T. Chu, J. C. Hu, F. S. Jeng, and R. J. Rau (2003). Active fault creep variations at Chihshang, Taiwan, revealed by creep mater monitoring, 1998–2001, *J. Geophys. Res.* **108,** no. B11, 2528, doi 10.1029/2003JB002394.

Ramsey, C. B. (1995). Radiocarbon calibration and analysis of stratigraphy: the OxCal program, *Radiocarbon* **37,** no. 2, 425–430.

Ramsey, C. B. (2001). Development of the Radiocarbon Program OxCal, *Radiocarbon* **43,** no. 2A, 355–363.

Ramsey, C. B. (2007). Radiocarbon calibration and analysis of stratigraphy: the OxCal Program 4.0.5, http://www.rlaha.ox.ac.uk/oxcal (last accessed July 2007).

Rau, R. J., and F. T. Wu (1998). Active tectonics of Taiwan orogeny from focal mechanisms of small-to-moderate-sized earthquakes, *Terr. Atmos. Ocean. Sci.* **9,** 755–778.

Reimer, P. J., M. G. L. Baillie, E. Bard, A. Bayliss, J. W. Beck, C. J. H. Bertrand, P. G. Blackwell, C. E. Buck, G. S. Burr, K. B. Cutler, P. E. Damon, R. L. Edwards, R. G. Fairbanks, M. Friedrich, T. P. Guilderson, A. G. Hogg, K. A. Hughen, B. Kromer, F. G. McCormac, S. W. Manning, C. B. Ramsey, R. W. Reimer, S. Remmele, J. R. Southon, M. Stuiver, S. Talamo, F. W. Taylor, J. van der Plicht, and C. E. Weyhenmeyer (2004). IntCal04 terrestrial radiocarbon age calibration, 26-0 ka BP, *Radiocarbon* **46,** 1029–1058.

Seno, T. (1977). The instantaneous rotation vector of the Philippine Sea plate relative to the Eurasian plate, *Tectonophysics* **42,** 209–226.

Shyu, J. B. H., L. H. Chung, Y. G. Chen, J. C. Lee, and K. Sieh (2007). Reevaluation of the surface ruptures of the November 1951 earthquake series in eastern Taiwan, and its neotectonic implications, *J. Asian Earth Sci.* **31,** 317–331.

Shyu, J. B. H., K. Sieh, J. P. Avouac, W. S. Chen, and Y. G. Chen (2006). Millennial slip rate of the Longitudinal Valley fault from river terraces: Implications for convergence across the active suture of eastern Taiwan, *J. Geophys. Res.* **111,** B08403, doi 10.1029/2005JB003971.

Shyu, J. B. H., K. Sieh, Y. G. Chen, and C. S. Liu (2005). Neotectonic architecture of Taiwan and its implications for future large earthquake, *J. Geophys. Res.* **110,** B08402, doi 10.1029/2005JB003251.

Taiwan Weather Bureau (1952). *The 1951 Earthquake Report*, Taiwan Weather Bureau, Taipei, 83 pp. (in Chinese).

Teng, L. S. (1990). Geotectonic evolution of Late Cenozoic arc-continent collision in Taiwan, *Tectonophysics* **183,** 57–76.

Teng, L. S. (1996). Extensional collapse of the northern Taiwan mountain belt, *Geology* **24,** 945–952.

Tsai, Y. B. (1986). Seismotectonics of Taiwan, *Tectonophysics* **125,** 17–37.

Wang, Y., and W. S. Chen (1993). Geological map of eastern Coastal Range, Central Geological Survey, scale 1:100,000.

Wells, D. L., and K. J. Coppersmith (1994). New empirical relationships among magnitude, rupture length, rupture width, rupture area and surface displacement, *Bull. Seismol. Soc. Am.* **84,** 974–1002.

Wu, F. T. (1978). Recent tectonics of Taiwan, *J. Phys. Earth* **26,** S265–S299.

York, J. E. (1976). Quaternary faulting in eastern Taiwan, *Bull. Geol. Surv. Taiwan* **25,** 63–72.

Yu, S. B., and L. C. Kuo (2001). Present-day crustal motion along the Longitudinal Valley fault, eastern Taiwan, *Tectonophysics* **333,** 199–217.

Yu, S. B., and C. C. Liu (1989). Fault creep on the central segment of the Longitudinal Valley fault, eastern Taiwan, *Proc. Geol. Soc. China* **32,** 209–231.

Yu, S. B., and Y. B. Tsai (1982). A study of microseismicity and crustal deformation of the Kungfu-Fuli area in eastern Taiwan, *Bull. Inst. Earth Sci., Acad. Sin.* **2,** 1–18.

Yu, S. B., H. Y. Chen, and L. C. Kuo (1997). Velocity field of GPS stations in the Taiwan area, *Tectonophysics* **274,** 41–59.

Yu, S. B., D. D. Jackson, G. K. Yu, and C. C. Liu (1990). Dislocation model for crustal deformation in the Longitudinal Valley area, eastern Taiwan, *Tectonophysics* **183,** 97–109.

Department of Geosciences
National Taiwan University
Taipei, Taiwan
d93224004@ntu.edu.tw
(I.-C.Y., W.-S.C., C.-C.B.Y., N.-W.H.)

Central Geological Survey (MOEA)
Taipei, Taiwan
(C.-W.L.)

Manuscript received 5 May 2007